

## 17.6 $\phi_1$ , or $\beta$

### Editors:

Chih-hsiang Cheng (BABAR)

Yoshihide Sakai (Belle)

Ikaros Bigi (theory)

### Additional section writers:

Tagir Aushev, Eli Ben-Haim, Adrian Bevan, Bob Cahn, Chunhui Chen, Ryosuke Itoh, Alfio Lazzaro, Owen Long, Fernando Martinez-Vidal, Vincent Poireau, Klaus Schubert

Precision measurement of the  $CP$  asymmetries in  $B \rightarrow J/\psi K_S^0$  decays was the principal motivation for building the  $B$  Factories. With the accumulation of data samples larger than anticipated, the BABAR and Belle experiments at the  $B$  Factories are able to study  $CP$  asymmetries in a wide range of related channels. This section describes measurements of the Unitarity Triangle angle  $\phi_1$ , also known as  $\beta$  in the literature. An overview of  $\phi_1$  measurements and their motivation is presented in Section 17.6.1, followed by a review of the quark transitions and the formalism of  $\phi_1$  measurements in Section 17.6.2. The various channels for  $\phi_1$  measurement, and the  $B$  Factories results, are then described in Sections 17.6.3–17.6.7. Resolution of discrete ambiguities is discussed in Section 17.6.8, and a summary of  $\phi_1$  results is presented in Section 17.6.10.

In the Standard Model, non-zero asymmetries measured in these analyses reflect violation of both the  $CP$  and  $T$  symmetries. Performing the measurement in a way that directly demonstrates  $T$  violation, without assuming (for example)  $CPT$  symmetry, requires special care. Such an analysis has been performed at BABAR, and is presented in Section 17.6.9. Tests of  $CPT$  symmetry are presented in Section 17.5.

### 17.6.1 Overview of $\phi_1$ measurement at the $B$ Factories

Initially,  $CP$  violation seemed isolated from the mainstream of particle physics. Since it was seen only in the  $K_S^0$ - $K_L^0$  system, it was possible to imagine that it was due entirely to a  $\Delta S = 2$  operator as postulated in the superweak theory (Wolfenstein, 1964). Two developments put  $CP$  violation at center stage. The first was A. D. Sakharov's demonstration (Sakharov, 1967) that  $CP$  violation was one of the three requirements for the existence of the baryon anti-baryon asymmetry of the universe (see Section 16.2). The second was Kobayashi's and Maskawa's demonstration that  $CP$  violation was natural if there were three generations of quarks (see Chapter 16). With the subsequent discovery of the last three quarks, testing the CKM model became urgent.

The  $K_S^0$ - $K_L^0$  system was not sufficient by itself to test the CKM picture. The measured parameters,  $\Delta m_K$ ,  $\epsilon_K$  and  $\epsilon'_K$ , depended not just on the fundamentals of the weak interactions, but on non-perturbative hadronic matrix elements. Moreover,  $CP$  violation in the kaon system

was feeble. Since  $\epsilon_K$  was measured in 1964, it took until 1973 before Kobayashi and Maskawa provided a real theory for  $CP$  violation. It needed many years to demonstrate that the parameter  $\epsilon'$  was non-zero. Even *before* the unexpected 'long' lifetime of  $B$  mesons was discovered, the  $B$  meson system was recognized as the ideal testing ground for  $CP$  violation (Bigi and Sanda, 1981) and the decay  $B \rightarrow J/\psi K_S^0$  as ideal for the purpose. Detection of the final state is especially clean because the  $J/\psi$  decays to lepton pairs and the  $K_S^0$  is sufficiently long-lived to decay into pairs of oppositely charged pions at a secondary vertex displaced from the interaction region.

Unlike neutral kaons, the neutral  $B$  mesons start oscillating just after their production, since their mixing rate  $\Delta m_d$  is comparable to their natural widths  $\Gamma$  (see Section 17.5). If we begin with a  $B^0$ , at a later time the state will be a superposition of  $B^0$  and  $\bar{B}^0$ . The decay to  $J/\psi K_S^0$  will occur through both components and the interference pattern will depend on the relative phases between the  $B^0$  and  $\bar{B}^0$  components, which is directly calculable in the CKM model. The interference pattern depends on the two decay amplitudes to the final state. Because the final state is a  $CP$  eigenstate and because there is only one significant pathway to it from  $B^0$  or  $\bar{B}^0$ , the two decay amplitudes are identical, up to another calculable phase. As a result, the oscillation pattern can be predicted simply in terms of the phases due to the CKM matrix without any dependence on hadronic physics. The time-dependent formalism required for the measurement of  $\sin 2\phi_1$  can be found in Chapter 10.

In order to test the CKM paradigm we need to know if we are starting with a  $B^0$  or with a  $\bar{B}^0$ . The  $\Upsilon(4S)$  is very near the threshold for  $B\bar{B}$  so if one  $B$  is observed, the remaining particles must come from another  $B$ . Moreover, by Bose symmetry, if a  $\bar{B}^0$  is observed the other particle must be a  $B^0$  at that instant, since the two mesons must be in an antisymmetric state to produce the unit of angular momentum carried by the  $\Upsilon(4S)$ . Thus "tagging" one  $B$  meson tells us both, when to start the clock and the type of  $B$  at that time (see Chapter 8).

The decay  $B^0 \rightarrow J/\psi K_S^0$  is just one of a large family of related decays due to a  $b \rightarrow c\bar{c}s$  transition. Of particular interest is the decay to  $J/\psi K_L^0$  because the final state has the opposite  $CP$  eigenvalue, and we expect exactly the opposite oscillation. Other charmonia can take the place of  $J/\psi$ , including  $\psi(2S)$ ,  $\eta_c$ , and  $\chi_{c1}$ . The decay  $B^0 \rightarrow J/\psi K^{*0}$  is more complex because the spins of the final state particles can be combined to produce an overall spin equal to 0, 1, or 2, and correspondingly the orbital angular momentum will be 0, 1, or 2. This complexity has the advantage that it can help resolve the ambiguity inherent in determining the angle  $\phi_1$  when only  $\sin 2\phi_1$  is known.

At first, the  $B$  Factories concentrated on measuring time-dependent asymmetries in the so-called charmonium "golden modes" concentrating on  $B^0 \rightarrow J/\psi K_S^0$ ,  $\psi(2S)K_S^0$ ,  $\chi_{c1}K_S^0$ ,  $J/\psi K_L^0$ , and  $J/\psi\pi^0$ . However, it was understood that there were other ways to measure  $\phi_1$ . Once an understanding of how to do these measurements started to develop, the experiments branched out to study similar

final states that were more difficult to isolate from the data. These states either had smaller branching fractions, or were experimentally more challenging to isolate. Studies performed in the *BABAR* physics book (Harrison and Quinn, 1998), prior to the commencement of data taking, assumed that a data sample of  $30 \text{ fb}^{-1}$  would be available to use for testing the SM. In reality this data sample was quickly attained on both sides of the Pacific Ocean and the *B* Factories program of measuring  $\phi_1$  expanded, both in terms of the number of measurements and in terms of the complexity of analysis used, to accommodate the rich harvest of *B* meson pairs. The first results on the measurement of  $\sin 2\phi_1$  were shown at the International Conference on High Energy Physics in 2000, which became known colloquially within *BABAR* and Belle as ‘the Osaka conference’. The *B* Factories presented values of  $\sin 2\phi_1$  of  $0.12 \pm 0.37 \pm 0.09$  (Aubert, 2000) and  $0.45^{+0.43}_{-0.44} {}^{+0.07}_{-0.09}$  (Aihara, 2000a) at this conference. A year later Belle and *BABAR* established large *CP* asymmetry in this final state. Since then both *B* Factories have accumulated much larger data samples, and the final results obtained by *BABAR* and Belle are significantly more precise than these first measurements (see Section 17.6.3).

While the charmonium decays were the primary focus of the  $\phi_1$  program, final states mediated by other transitions were also studied in subsequent waves of measurements that quickly followed the first results. In particular the modes  $\bar{B} \rightarrow \phi K_s^0$ ,  $B \rightarrow \eta' K_s^0$ , and  $D^{(*)+} D^{(*)-}$  were highlighted. The expectation was that these would provide alternative ways of constraining  $\phi_1$ , and would complement the constraint on the Unitarity Triangle given by the golden mode measurements. Any measurement of  $\phi_1$  that differed significantly from expectations, or any two measurements that disagreed with each other, could reveal physics beyond the Standard Model.

The first few measurements of  $S \simeq \sin(2\phi_1)$  in a quasi-two-body analysis of  $B \rightarrow \phi K_s^0$  decays in 2003 were far from the SM expectation. While these were low statistics studies, with only a handful of high purity events (well tagged events with a low mistag probability, see Chapter 8), the community was tantalized by the possibility that this could herald a new age in modern physics. As a result, the interest in alternative measurements of  $\phi_1$  blossomed, and this remains a vibrant area a decade later. Alas, the early deviations from the SM turned out to be statistical fluctuations, and the most recent measured values of  $\phi_1$  obtained from the *B* Factories are compatible with SM expectations within experimental and theoretical uncertainties.

The early fluctuation had several consequences. First, a large number of neutral *B* meson decays to *CP* eigenstate or admixture final states have been studied in the hope that one or more of them might yield a result incompatible with the SM. Second, both the theoretical and experimental communities started to take possible hadronic uncertainties more seriously in both golden and alternative measurements of  $\phi_1$ . Today the constraints on hadronic uncertainties in these modes are a mixture of theoretical calculations and data-driven constraints obtained

via a more phenomenological approach. The golden channels are theoretically clean, up to the extent that analysis at the *B* Factories would be concerned about. This has been determined via theoretical calculation, and via a data-driven interpretation of results. However other final states, in particular those dominated by penguin loop amplitudes, have non-negligible uncertainties. The cleanest modes are  $B \rightarrow \eta' K_s^0$ , which is the most precisely measured charmless final state, and  $B \rightarrow \phi K_s^0$ . These have hadronic uncertainties of a few percent on the measured value of  $S$ . In the case of  $B \rightarrow f_0 K_s^0$  there are only partial calculations where, for example, long distance effects are ignored, and the estimated hadronic uncertainties for this mode provide a lower bound. More details on this part of the *B* Factory program can be found in Section 17.6.6.

Early time-dependent studies of *B* decays to charmless final states relied on a simplified analysis paradigm by imposing the quasi-two-body assumption that resonances are particles of definite mass, so that interference between amplitudes could be neglected. As the recorded data samples of the two experiments increased, more sophisticated techniques were incorporated. Just as the measurements of  $\phi_2$  ultimately required that the *B* Factories pioneer the use of time-dependent Dalitz plot techniques, so eventually one had to perform similar analyses in order to constrain  $\phi_1$ . The ability to study amplitudes in a Dalitz plot leads to the possibility of resolving the four-fold ambiguity in the value of  $\phi_1$  obtained from the golden mode measurement, and complements other approaches such as the full angular analysis of the  $B^0 \rightarrow J/\psi K^*$  final state. Results from three-body charmless decays on  $\phi_1$  are discussed in Section 17.6.7, and resolution of discrete ambiguities on the value of this angle using other modes is considered in Section 17.6.8.

The large amounts of data accumulated by the *B* Factories also required an improvement in understanding the systematic uncertainties involved in the measurements themselves. In particular the concept of flavor tagging as originally conceived, while good enough to describe semi-leptonic tagged events, turned out to be an approximation for hadronically tagged final states. It is possible to have a small level of *CP* violation manifest on the tag side of the event that would need to be considered as a systematic uncertainty in order to ensure that one reports the correct level of *CP* violation obtained for a given result. In some cases with small expected *CP* violating asymmetries, such as the measurement of  $\sin(2\phi_1 + \phi_3)$ , this so-called tag-side interference needs to be incorporated into the measurement technique. The main systematic uncertainties for time-dependent measurements at the *B* Factories, including tag-side interference, are discussed in Chapter 15.

The final measurement of  $\sin 2\phi_1 \equiv \sin 2\beta$  obtained by the *B* Factories has a combined precision of 3%. This can be compared with the estimated relative statistical precision for this measurement estimated in the *BABAR* physics book, 12%, using a foreseen data sample of  $30 \text{ fb}^{-1}$  (Harrison and Quinn, 1998). The achieved precision is a nice example of exceeding the initial expectations put forward before the startup of the *B* Factories. The final result of

the  $B$  Factories is not systematically limited and may be improved upon by the next generation of experiments.

### 17.6.2 Transitions and formalism

The Unitarity Triangle angle  $\phi_1 = \beta$  is defined as

$$\phi_1 \equiv \beta \equiv \arg[-(V_{cd}V_{cb}^*)/(V_{td}V_{tb}^*)]. \quad (17.6.1)$$

It describes  $CP$  violation in the interference between decays with and without  $B^0$ - $\bar{B}^0$  mixing and is best measured in  $B^0 \rightarrow J/\psi(\psi(2S))K_s^0$  transitions, which have  $CP$ -odd final states (ignoring the small  $CP$  violation in  $K^0$ - $\bar{K}^0$  mixing). As discussed in Section 10.1,  $\Delta B = 2$  transitions in the SM are produced by quark box diagrams  $O_{\text{box}}$  including QCD radiative corrections for  $\Delta m_d$ .

The most precise technique for measuring  $\phi_1$  uses  $B^0$  decays to  $CP$  eigenstates with quark transitions of the type  $b \rightarrow c\bar{c}s$  (Fig. 17.6.1). Since the final state  $f$  is accessible to both  $B^0$  and  $\bar{B}^0$ , the amplitudes for  $B^0 \rightarrow f$  (direct decay) and  $B^0 \rightarrow \bar{B}^0 \rightarrow f$  (decay preceded by neutral meson oscillation) will interfere. As described in Section 10.2,<sup>70</sup> the resulting time-dependent  $CP$  asymmetry is given as

$$A(\Delta t) = S \sin(\Delta m_d \Delta t) - C \cos(\Delta m_d \Delta t), \quad (17.6.2)$$

where  $S = 2\text{Im}\lambda/(1 + |\lambda|^2)$ ,  $C = (1 - |\lambda|^2)/(1 + |\lambda|^2)$ , and  $\lambda = (q/p)(\bar{A}_f/A_f)$ . In the SM,  $q/p = V_{td}V_{tb}^*/V_{\bar{t}d}V_{\bar{t}b}$  to a good approximation. For the final state  $f = J/\psi K_s^0$ , the  $B$  decay is dominated by a tree  $b \rightarrow c\bar{c}s$  (or its  $CP$  conjugate) amplitude<sup>71</sup> followed by  $K^0$ - $\bar{K}^0$  mixing.<sup>72</sup> The result is  $\lambda = \eta_f \frac{V_{td}V_{tb}^* V_{cb}V_{cd}^*}{V_{\bar{t}b}V_{\bar{t}d}^* V_{cd}V_{cb}^*}$ , which leads to  $C = 0$  and  $S = -\eta_f \sin 2\phi_1$ , where  $\eta_f = \eta_{J/\psi K_s^0} = -1$  is the  $CP$  eigenvalue.  $B^0 \rightarrow J/\psi K_L^0$  has  $\eta_f = \eta_{J/\psi K_L^0} = +1$  and has the opposite sign for  $S$ . The same magnitude is expected for the  $CP$ -even and -odd modes up to a small correction for  $CP$  violation in  $K^0$ - $\bar{K}^0$  oscillations.

To understand the penguin amplitude contributions, one can group tree ( $T$ ) and penguin ( $P^q$ ) amplitudes according to their CKM factors, remove the  $V_{tb}V_{ts}^*$  term using the unitarity condition

$$\sum_{q=u,c,t} V_{qb}V_{qs}^* = 0, \quad (17.6.3)$$

and express the  $b \rightarrow c\bar{c}s$  decay amplitude as

$$A_{c\bar{c}s} = V_{cb}V_{cs}^*(T + P^c - P^t) + V_{ub}V_{us}^*(P^u - P^t), \quad (17.6.4)$$

where the superscripts indicate the quark in the loop. The second term has a different phase but the magnitude is suppressed by  $|V_{ub}V_{us}^*/V_{cb}V_{cs}^*| \sim \mathcal{O}(\lambda_{\text{Cabibbo}}^2)$ . Therefore, the effect of the penguin amplitude on  $\phi_1$  is expected to be very small.

<sup>70</sup> See in particular Eqs (10.2.2, 10.2.4, 10.2.4, and 10.1.10).

<sup>71</sup>  $B$  decay amplitude ratio provides a factor  $\eta_f \frac{V_{cb}V_{cs}^*}{V_{\bar{c}b}V_{\bar{c}s}^*}$ .

<sup>72</sup>  $K^0$ - $\bar{K}^0$  mixing provides a factor  $V_{cd}^*V_{cs}/V_{cd}V_{cs}^*$ .

Within the SM the level of  $CP$  violation in decay ( $|A_f/\bar{A}_f| \neq 1$ ) is expected to be inaccessible to existing experiments, and new physics (NP) beyond the SM is unlikely to generate large effects due to the dominance of the tree amplitude in decay. However, NP could modify the time-dependent  $CP$  asymmetry across different modes by affecting the phase in  $q/p$  and lead to inconsistencies between  $\phi_1$  and other observables that determine the Unitarity Triangle.

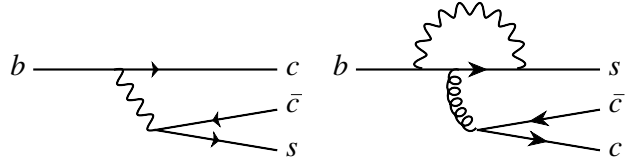


Figure 17.6.1. Tree and penguin diagrams of  $b \rightarrow c\bar{c}s$ .

In  $b \rightarrow c\bar{c}d$  (Fig. 17.6.2) decays, the difference between the CKM phase of the tree diagram and that of  $b \rightarrow c\bar{c}s$  is negligible. This allows the measurements of  $\sin 2\phi_1$  through decays to  $CP$  eigenstates of  $b \rightarrow c\bar{c}d$  (such as  $B^0 \rightarrow J/\psi \pi^0$  and  $D^+ D^-$ ) in the same way as  $b \rightarrow c\bar{c}s$ . Unlike  $b \rightarrow c\bar{c}s$ , however, the CKM factors of the penguin diagrams here are of the same order ( $\mathcal{O}(\lambda_{\text{Cabibbo}}^3)$ ) as the tree diagram. The possible contribution of the  $b \rightarrow c\bar{c}d$  penguin diagrams, which have a different CKM phase, can alter the measured value of  $\sin 2\phi_1$ . Any such deviation would be due to the effect of penguin contributions or due to NP.

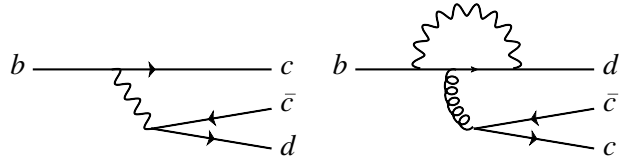


Figure 17.6.2. Tree and penguin diagrams of  $b \rightarrow c\bar{c}d$ .

The  $b \rightarrow c\bar{u}d$  transition (Fig. 17.6.3) proceeds through a tree diagram, and has no penguin contribution. It can again be used to probe  $\sin 2\phi_1$  if the final state is accessible to both  $B^0$  and  $\bar{B}^0$  (e.g., in the case of intermediate  $D^0$  and  $\bar{D}^0$  decays to the same final state). However, in this case, the process  $b \rightarrow u\bar{c}d$  also contributes. The relative CKM factor of these two tree diagrams,  $V_{ub}V_{cd}^*/V_{cb}V_{ud}^*$ , has a large phase and the magnitude is approximately 0.02. Therefore, the deviation from the  $b \rightarrow c\bar{c}s$  value for  $\sin 2\phi_1$  obtained in these decays is expected to be small.

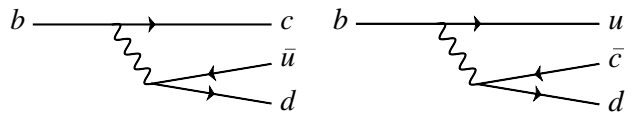
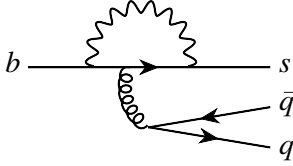


Figure 17.6.3. Tree diagrams of  $b \rightarrow c\bar{u}d$  and  $b \rightarrow u\bar{c}d$ .

The decays to  $CP$  eigenstates dominated by  $b \rightarrow s\bar{q}q$  penguin transitions (Fig. 17.6.4) also can be used for  $\sin 2\phi_1$  measurements in the SM. Similar to Eq. (17.6.4), the dominant penguin contribution has the same phase as that in the  $b \rightarrow c\bar{c}s$  tree diagram, and the sub-dominant term is suppressed. Any deviation of  $S$  from the  $b \rightarrow c\bar{c}s$  decay (beyond theoretical uncertainty) is a clear indication of the effect of NP. The decays proceeding via  $b \rightarrow s\bar{s}s$  penguin diagrams, such as  $B^0 \rightarrow \phi K^0$ ,  $K_s^0 K_s^0 K_s^0$ , and  $\eta' K^0$ , have a small theoretical uncertainty on  $S$  due to the lack of a tree amplitude contribution. These decays are particularly promising for future new physics searches.



**Figure 17.6.4.** Penguin diagram of  $b \rightarrow q\bar{q}s$ .

Measurements of  $\sin 2\phi_1$  have a four-fold ambiguity in  $\phi_1$ :  $\phi_1 \leftrightarrow \pi/2 - \phi_1$ ,  $\phi_1 + \pi$  and  $3\pi/2 - \phi_1$  (all these four values result in the same  $\sin 2\phi_1$ ). The  $\phi_1 \leftrightarrow \pi/2 - \phi_1$  and  $3\pi/2 - \phi_1$  ambiguity can be resolved in one of several ways: the full time-dependent angular analysis of vector-vector final states such as  $B^0 \rightarrow J/\psi K^{*0}[K_s^0\pi^0]$ ; time-dependent Dalitz analysis of three-body decays; time-dependent Dalitz analysis of  $D^0 \rightarrow K_s^0\pi^+\pi^-$  in  $B^0 \rightarrow D^{(*)0}h^0$ ; and time-dependent measurements in two separate Dalitz regions in  $B^0 \rightarrow D^{*+}D^{*-}K^0$ . Using these measurements the ambiguity is partially resolved and only the two fold ambiguity  $\phi_1 \rightarrow \phi_1 + \pi$  remains, which cannot be resolved by a single measurement. When combining with other CKM measurements, one can clearly see which of the two remaining solutions is ruled out. See Chapter 25 for details.

The following sections describe the different measurements of  $\phi_1$  made at the  $B$  Factories.

### 17.6.3 $\phi_1$ from $b \rightarrow c\bar{c}s$ decays

The decays to  $CP$  eigenstates via a  $b \rightarrow c\bar{c}s$  transition include  $B^0$  decays to charmonium ( $c\bar{c}$ ) and a  $K_s^0$  or  $K_L^0$ . These modes have experimentally clean signals, and large signal yields are expected due to relatively large branching fractions (they are CKM favored, though color suppressed<sup>73</sup>). These decays are also theoretically very clean for  $\phi_1$  determination, *i.e.*, the deviation due to the contribution of penguin diagrams with a different CKM phase is expected to be at the  $\leq 1\%$  level (H. Boos and Reuter,

<sup>73</sup> Each of the two quarks ( $\bar{c}s$ ) from the virtual  $W$  is paired with the quark originating from the initial state ( $b\bar{d}$ ) to form a hadron. Since hadrons have to stay color-neutral, the color of  $\bar{c}$  and  $s$  must match that of  $b$  and  $\bar{d}$ . Therefore the overall amplitude is  $1/\text{number-of-colors}$  smaller than the decays in which  $W^* \rightarrow \bar{q}q'$  hadronize by themselves.

2004, 2007). As a result the  $B^0 \rightarrow J/\psi K_s^0$  decay is called a “Golden mode”.

Since the observation of  $CP$  violation in  $B$  decays and the precise measurements of  $\sin 2\phi_1$  are the primary goals of the asymmetric  $B$  Factories, the measurements made using  $b \rightarrow c\bar{c}s$  modes were performed shortly after data taking commenced, and have been updated several times during the course of data taking. Both  $B$  Factories have updated their measurements using the whole data sample collected by each experiment. *BABAR* (Aubert, 2009z) uses  $465 \times 10^6 B\bar{B}$ , while *Belle* (Adachi, 2012c) uses  $772 \times 10^6 B\bar{B}$  pairs. For  $\phi_1$  measurements with  $b \rightarrow c\bar{c}s$  decays, the  $B^0$  decays to the final states  $J/\psi K_s^0$ ,  $J/\psi K_L^0$ ,  $\psi(2S)K_s^0$ ,  $\chi_{c1}K_s^0$ ,  $\eta_c K_s^0$ , and  $J/\psi K^*(890)^0[K_s^0\pi^0]$  are used. The  $J/\psi K_L^0$  state is  $CP$ -even, and  $J/\psi K^*(890)^0$  is an admixture of two  $CP$  states. All the others are  $CP$ -odd states.

The  $J/\psi$  and  $\psi(2S)$  mesons are reconstructed via their decays to  $\ell^+\ell^-$  ( $\ell = e, \mu$ ). For decays to an  $e^+e^-$  final state, photons near the direction of the  $e^\pm$  are added to recover the energy lost by radiated bremsstrahlung. The  $\psi(2S)$  mesons are also reconstructed in the  $J/\psi\pi^+\pi^-$  final state. The  $\chi_{c1}$  mesons are reconstructed in the  $J/\psi\gamma$  final state, and these photons must not be consistent with photons from  $\pi^0$  decays. The  $\eta_c$  mesons are reconstructed in the  $K_s^0 K^+\pi^-$  final states, and the regions that contain the dominant intermediate resonant states in  $K^+\pi^-$  and  $K_s^0 K^+$  are selected. Candidate  $K_s^0$  mesons are reconstructed via decays to the  $\pi^+\pi^-$  final state. For the  $B^0 \rightarrow J/\psi K_s^0$  decay mode,  $K_s^0$  mesons are also reconstructed in the  $\pi^0\pi^0$  final state. Inclusion of the  $K_s^0 \rightarrow \pi^0\pi^0$  channel increases a signal yield by about 20% of the  $K_s^0 \rightarrow \pi^+\pi^-$  channel. The masses of  $J/\psi$ ,  $\psi(2S)$ ,  $\chi_{c1}$ , and  $K_s^0$  candidates are constrained to their respective nominal values to improve their momentum resolutions. Candidate  $K_L^0$  mesons are identified using information from the electromagnetic calorimeter and IFR/KLM detectors (see Chapter 2), requiring that the signals in these detectors are not associated with any charged tracks. Since the energy of a  $K_L^0$  cannot be measured precisely, only the flight direction is used when reconstructing  $B^0 \rightarrow J/\psi K_L^0$  decay candidates. The  $K^{*0}$  candidates are selected by combining  $K_s^0$  and  $\pi^0$  mesons. *BABAR* uses all of the aforementioned final states for their analysis. While *Belle* (Abe, 2001g) used the same set of modes for earlier iterations of their analysis, more recent updates do not include the  $J/\psi K_s^0(\rightarrow \pi^0\pi^0)$ ,  $\eta_c K_s^0$ , and  $J/\psi K^{*0}$  final states.

Candidate  $B^0$  mesons are reconstructed by combining charmonium and  $K_s^0$ ,  $K_L^0$ , or  $K^{*0}$  candidates. Two kinematic variables  $\Delta E$  and  $m_{ES}$  (see Section 7.1.1) are used to select signal candidates, with the exception of the  $B^0 \rightarrow J/\psi K_L^0$  channel. For the latter case a kinematic constraint is applied assuming a two-body decay of the  $B^0$ , and both *BABAR* and *Belle* use  $\Delta E$  and the momentum of the reconstructed  $B^0$  in the center-of-mass (CM) system ( $p_B^*$ ) to isolate signal candidates. Figure 17.6.5 shows the  $m_{ES}$  and  $\Delta E$  distributions for candidates satisfying the flavor tagging and vertex reconstructions in the *BABAR*

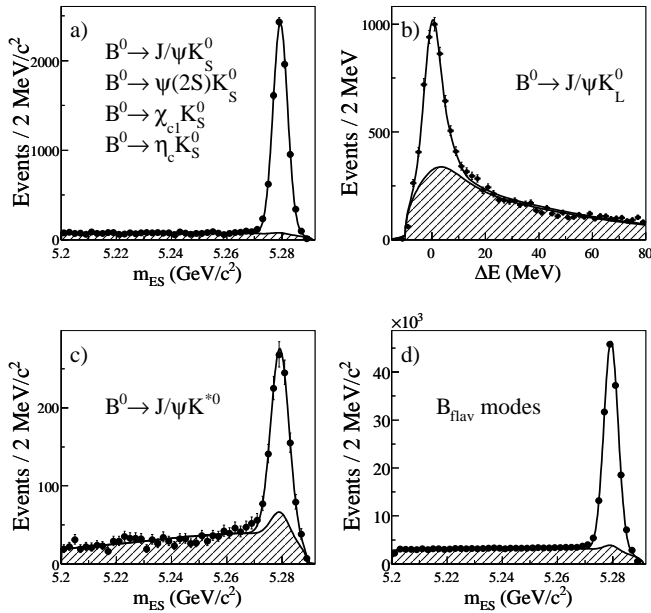


**Figure 17.6.5.** Distributions of  $m_{ES}$  or  $\Delta E$  for (a)  $B^0 \rightarrow (c\bar{c})K_S^0$ , (b)  $B^0 \rightarrow J/\psi K_L^0$ , (c)  $B^0 \rightarrow J/\psi K^{*0}$ , and (d)  $B^0$  decays to flavor-specific final states for the samples used in the BABAR measurement (Aubert, 2009z) of  $\phi_1$ . The shaded regions represent the estimated background, and the solid lines are the projections of the fits to the data.

analysis. Figure 17.6.6 shows the  $m_{ES}$  and  $p_B^*$  distributions for the Belle analysis.

Vertex reconstruction and  $B$  meson flavor tagging algorithms (described in Chapters 6 and 8) are applied to the selected signal candidates. Time-dependent  $CP$  asymmetry parameters are extracted from fits to the distributions of proper decay time difference between signal and tagged  $B$  mesons as described in Chapter 10. BABAR extracts the time-dependent asymmetry parameters ( $S$  and  $C$ ) from a simultaneous fit to both the  $B_{CP}$  and  $B_{flav}$  (see Section 10.2) samples with 69 additional free parameters, where tagging and resolution parameters are transparently propagated into the  $CP$  analysis as part of the final statistical error. Belle takes a multi-step approach: the final fit includes only  $S$  and  $C$  as free parameters, and all the fit model parameters, which include signal fractions, flavor tagging performance parameters, and proper time difference resolution function parameters are fixed to the values determined from separate fits to the  $B_{flav}$  and  $B_{CP}$  samples. Effects arising from the uncertainties of these parameters are included in the final result as systematic errors.

The results of the time-dependent  $CP$  asymmetry measurements are summarized in Table 17.6.1 for each decay mode, and for the combined set of modes. As described in Section 17.6.8, the time-dependent full angular analysis of the  $B^0 \rightarrow J/\psi K^{*0}$  decay can provide a value for  $\cos 2\phi_1$  in addition to  $\sin 2\phi_1$ . The angular information presented in the table has been averaged over, resulting in a dilution of the measured  $CP$  asymmetry by a fac-

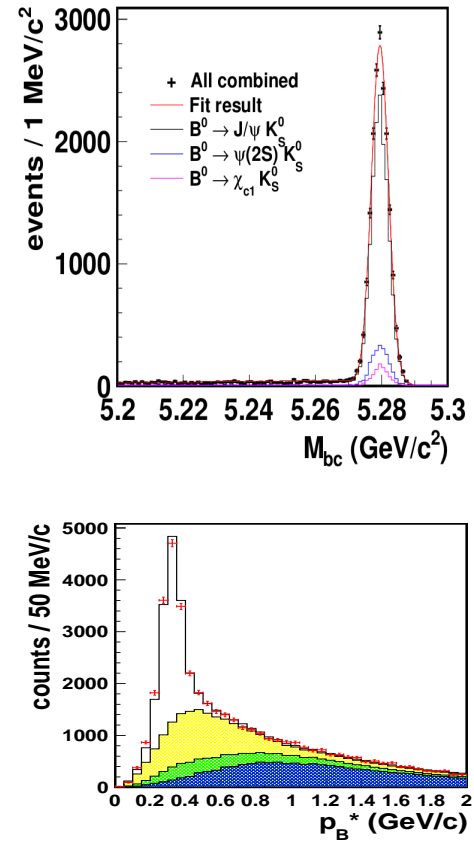


**Figure 17.6.6.** Distributions of  $m_{ES}$  ( $= M_{bc}$ ) for  $B^0 \rightarrow (c\bar{c})K_S^0$  (top) and  $p_B^*$  for  $B^0 \rightarrow J/\psi K_L^0$  (bottom) obtained with the samples used for the Belle measurement (Adachi, 2012c) of  $\phi_1$ . The shaded regions in the bottom plot represent the estimated background components: (from top to bottom) real  $J/\psi$  and real  $K_L^0$  (yellow), real  $J/\psi$  and fake  $K_L^0$  (green), and fake  $J/\psi$  (blue).

tor of  $1 - 2R_{\perp}$ , where  $R_{\perp}$  is the fraction of the  $CP$ -odd component. BABAR uses the previously measured value  $0.233 \pm 0.010 \pm 0.005$  (Aubert, 2007x). Systematic errors on the time-dependent asymmetry parameters are summarized in Table 17.6.2. The dominant sources for  $S$  are due to the uncertainties in vertex reconstruction and  $\Delta t$  resolutions, flavor tagging, and background in the  $J/\psi K_L^0$  mode. The systematic error on  $C$  is dominated by tag-side interference. For this source, Belle takes into account a cancellation between  $CP$ -even and  $CP$ -odd states, while BABAR does not. Chapter 15 discusses the main sources of systematic uncertainty on time-dependent  $CP$  asymmetry parameter measurements in detail.

The  $\Delta t$  distributions and asymmetries obtained from the data for all modes combined are shown in Fig. 17.6.7. The values of  $C$  obtained are consistent with zero in accordance with SM expectations, and hence  $-\eta_f S$  gives essentially  $\sin 2\phi_1$ . The average of the two experiments

**Table 17.6.1.** Summary of the time-dependent  $CP$ -asymmetry measurements using  $B^0$  decays to charmonium +  $K^0$  final states, for each decay mode and for all modes combined.  $N_{\text{tag}}$  and  $P$  are the number of candidates and signal purity (in %), respectively, in the signal region after flavor tagging and vertex reconstruction requirements have been applied.  $S$  and  $C$  are the  $CP$  asymmetry parameters for the final state with the  $CP$  eigenvalue  $\eta_f$ .

Mode	BABAR (Aubert, 2009z)				Belle (Adachi, 2012c)			
	$N_{\text{tag}}$	$P$	$-\eta_f S$	$C$	$N_{\text{tag}}$	$P$	$-\eta_f S$	$C$
$J/\psi K_S^0$	6750	95	$0.657 \pm 0.036 \pm 0.012$	$0.026 \pm 0.025 \pm 0.016$	13040	97	$0.670 \pm 0.029 \pm 0.013$	$0.015 \pm 0.021$ $^{+0.023}_{-0.045}$
$J/\psi K_L^0$	5813	56	$0.694 \pm 0.061 \pm 0.031$	$-0.033 \pm 0.050 \pm 0.027$	15937	63	$0.642 \pm 0.047 \pm 0.021$	$-0.019 \pm 0.026$ $^{+0.041}_{-0.017}$
$\psi(2S)K_S^0$	861	87	$0.897 \pm 0.100 \pm 0.036$	$0.089 \pm 0.076 \pm 0.020$	2169	91	$0.738 \pm 0.079 \pm 0.036$	$-0.104 \pm 0.055$ $^{+0.027}_{-0.047}$
$\chi_{c1}K_S^0$	385	88	$0.614 \pm 0.160 \pm 0.040$	$0.129 \pm 0.109 \pm 0.025$	1093	86	$0.640 \pm 0.117 \pm 0.040$	$0.017 \pm 0.083$ $^{+0.026}_{-0.046}$
$\eta_c K_S^0$	381	79	$0.925 \pm 0.160 \pm 0.057$	$0.080 \pm 0.124 \pm 0.029$				
$J/\psi K^{*0}$	1291	67	$0.601 \pm 0.239 \pm 0.087$	$0.025 \pm 0.083 \pm 0.054$				
All	15481	76	$0.687 \pm 0.028 \pm 0.012$	$0.024 \pm 0.020 \pm 0.016$	32239	79	$0.667 \pm 0.023 \pm 0.012$	$-0.006 \pm 0.016 \pm 0.012$

**Table 17.6.2.** Summary of systematic errors on the time-dependent  $CP$  asymmetry parameters measured in  $B^0$  decays to charmonium +  $K^0$  for all modes combined.

Source	BABAR		Belle	
	$S$	$C$	$S$	$C$
Vertex and $\Delta t$	0.007	0.003	0.010	0.007
Flavor tagging	0.006	0.002	0.004	0.003
$J/\psi K_L^0$ background	0.006	0.001	0.004	0.002
Other signal/background	0.005	0.003	0.002	0.001
Physics parameters	0.003	0.001	0.001	0.000
Tag-side interference	0.001	0.014	0.001	0.008
Possible fit bias	0.002	0.003	0.004	0.005
Total	0.012	0.016	0.012	0.012

(Amhis et al., 2012) gives

$$\sin 2\phi_1 = 0.677 \pm 0.020 \quad \text{and} \quad C = 0.006 \pm 0.017. \quad (17.6.5)$$

This corresponds to  $\phi_1 = (21.30 \pm 0.78)^\circ$  (up to the four-fold ambiguity mentioned above). An accuracy of 3% on  $\sin 2\phi_1$  ( $0.8^\circ$  on  $\phi_1$ ) is achieved.

The evolution of the measured value of  $\sin 2\phi_1$  can be seen in Fig. 17.6.8. Central values for the initial measurements from both experiments were slightly lower than the current world average. A significant milestone in the measurement of  $\sin 2\phi_1$  was achieved in the summer of 2001 when both *BABAR* and Belle observed  $CP$  violation in  $B^0$  meson decay.<sup>74</sup> The data samples used for these measurements each consists of about  $30 \times 10^6 B\bar{B}$  pairs. Since that time, improved measurements have proved to be stable, and the results reported by *BABAR* and Belle have remained consistent with each other.

## 17.6.4 $\phi_1$ from $b \rightarrow c\bar{c}d$ decays

### 17.6.4.1 $B^0 \rightarrow J/\psi\pi^0$

The decay  $B^0 \rightarrow J/\psi\pi^0$  is a  $b \rightarrow c\bar{c}d$  transition into a  $CP$ -even final state. The final state has contributions from both a color- and Cabibbo-suppressed tree amplitude, and penguin amplitudes with different weak phases. In the absence of penguin contributions one can measure the Unitarity Triangle angle  $\phi_1$  using this decay. If there are significant penguin contributions, the measured value of  $\phi_1$ , called the “effective phase”  $\phi_1^{\text{eff}}$ , may differ from that obtained from the tree-dominated  $B \rightarrow J/\psi K^0$  decays. There are two motivations for such a measurement; firstly it is possible to constrain theoretical uncertainties in  $B \rightarrow J/\psi K^0$  decays using  $B^0 \rightarrow J/\psi\pi^0$  (Ciuchini, Pierini, and Silvestrini, 2005), and secondly one may be able to probe, or constrain, possible new physics contributions to  $b \rightarrow c\bar{c}d$  transitions manifesting via loop diagrams.

<sup>74</sup> A commonly accepted definition of “observation” is a result with a statistical significance of at least five standard deviations if the uncertainties are treated as Gaussian.

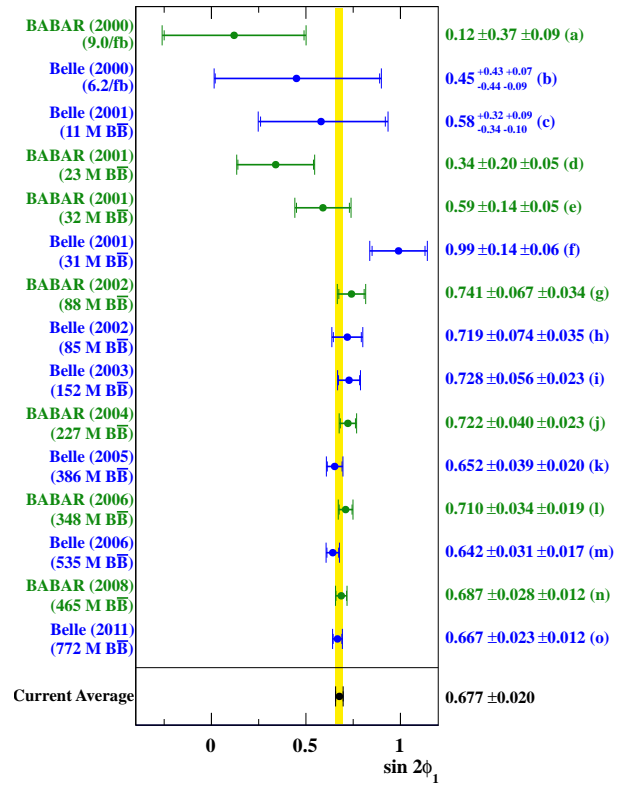


**Figure 17.6.8.** History of the  $\sin 2\phi_1$  measurements with  $b \rightarrow c\bar{c}s$  decays, ordered by the dates they appeared in public. References: (a) (Aubert, 2000), (b) (Aihara, 2000a), (c) (Abashian, 2001), (d) (Aubert, 2001a), (e) (Aubert, 2001e), (f) (Abe, 2001g), (g) (Aubert, 2002g), (h) (Abe, 2002b), (i) (Abe, 2005c), (j) (Aubert, 2005i), (k) (Abe, 2005j), (l) (Aubert, 2006j), (m) (Chen, 2007a), (n) (Aubert, 2009z), (o) (Adachi, 2012c).

Unlike  $b \rightarrow c\bar{c}s$  decays, which are experimentally clean, one has to consider significant background contributions when trying to extract information from  $B^0 \rightarrow J/\psi\pi^0$  signal events. These background contributions include events from  $B$  decays to  $J/\psi\rho^0$ ,  $J/\psi K_s^0$ ,  $J/\psi K^{*0}$ ,  $J/\psi K^{*\pm}$ , and  $J/\psi\rho^\pm$  final states as well as smaller contributions from other  $B$  decays to final states including a  $J/\psi$ . The aforementioned backgrounds populate the negative  $\Delta E$  region (peak  $\sim -0.2$  GeV) and have a tail in the signal region around  $\Delta E \sim 0$  (see Fig. 17.6.9). Since these modes are well measured, the  $B$  Factories have relied on existing branching fraction measurements from the Particle Data Group (Yao et al., 2006) in order to fix the normalization of background contributions while extracting signal yields and  $CP$  asymmetry parameters. The normalization of the combinatorial background is allowed to vary in the fit.

Both experiments perform an unbinned maximum likelihood fit to data using discriminating variables:  $m_{ES}$ ,  $\Delta E$ , and  $\Delta t$ . In order to suppress background from light-quark continuum events, *BABAR* also includes a Fisher discriminant as one of the discriminating variables in their fit to data. This is computed using three variables:  $L_0$ ,  $L_2$